

PRESSURE SIMULATIONS FOR THE EIC INTERACTION REGION*

M. L. Stutzman[†], Thomas Jefferson National Accelerator Facility, Newport News, VA, USA

Abstract

Background detector rates in the Electron Ion Collider depend in part on the pressure in the interaction region. Materials choice, synchrotron radiation induced desorption, conditioning time and pumping configuration all affect the pressure in the system. Simulations of the region using Synrad+ and Molflow+ coupled simulation codes will be presented for various configurations and conditioning times.

INTRODUCTION

The success of the US Electron Ion Collider (EIC) depends in part on the ability to manage detector background rates due to many sources [1]. This paper addresses sources of detector background due to synchrotron radiation directly incident on the interaction beampipe as well as vacuum-induced pressure rise in the interaction region, which affects background rates due to scattering events of the ion beam on the residual gasses in the beampipe.

INTERACTION REGION DESIGN

The EIC interaction region (IR) places many requirements on the beamline design. The EIC detector includes a central region magnet, layers of particle trackers surrounding the central IR, as well as Endcap detectors for particles which are scattered at small angles from the incident electron and ion beams. Additionally, the vacuum system for the IR must transition to the vacuum chambers and cryostats of the superconducting dipole and quadrupole magnets while considering impedance constraints [2].

The vacuum system consists of a long straight beampipe for the electron beam (Fig. 1), with the final dipole approximately 35 m upstream of the interaction point (IP). The distance between the final dipole and the IP allows much of the synchrotron radiation (SR) from the dipole to be absorbed before reaching the IR.

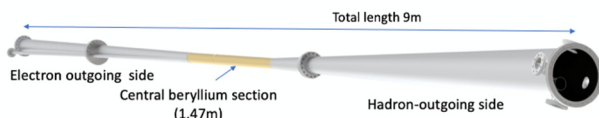


Figure 1: Interaction region vacuum chamber layout [1].

The ion beam travels in a straight path, crossing the electron beam at the IR with an angle of 25 mrad. The ion beam then exits through an opening in the incident electron beampipe into a conical vacuum chamber. The chamber

* This paper was authored by Jefferson Science Associates, LLC under U.S. DOE Contract No. DE-AC05-06OR23177.

[†] marcy@jlab.org

will interface with an endcap detector for particles scattered at far forward angles. The central beampipe will be fabricated from beryllium coated with approximately 2 μm of gold. Beryllium is chosen to reduce particle scattering and gold will absorb low energy synchrotron radiation. The remainder of the system is will be aluminum, which is a low-Z materials that has adequate thermal conductivity and can be easily fabricated.

SYNCHROTRON RADIATION SIMULATION

Synchrotron radiation generated by the electron beam passing through the last dipole and final quadrupole magnets has been modeled using the Synrad+ test-particle Monte Carlo code developed at CERN [3]. After importing a CAD model of the IR vacuum chamber and the incoming electron beamline, along with electron beam parameters and magnetic field maps, Synrad generates the synchrotron radiation flux and energy distribution on the various vacuum surfaces (see Fig. 2). Each photon reaching the surface of the vacuum chamber will be reflected or absorbed based on the photon energy and the material parameters, including surface roughness and chamber material. The simulated photons are tracked until they exit the simulation. The test particle Monte Carlo then scales the simulation statistically to compute the photon flux expected for a given beam current.

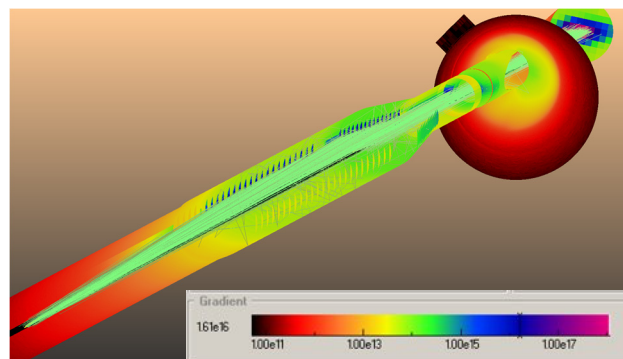


Figure 2: Synchrotron radiation flux distribution on the incoming electron beampipe, with flux gradient in photons/s/cm² shown in the scale.

The photon flux incident on the central beryllium section is of particular interest. Photons striking the Be pipe will generate undesirable detector backgrounds, and can damage the sensitive silicon vertex detector elements installed immediately adjacent to the beampipe. Therefore this synchrotron radiation flux must be modeled and mitigated.

Simulations of the photon flux for the central Be pipe have been made for various configurations. Figure 3 shows

Content from this work may be used under the terms of the CC BY 3.0 licence (© 2021). Any distribution of this work must maintain attribution to the author(s), title of the work, publisher, and DOI

the photon flux as a function of azimuthal angle and distance z along the beamline for a section of beamline. Fig. 3 shows a non-optimized system, and is used only to illustrate the simulations rather than to give an expected photon flux.

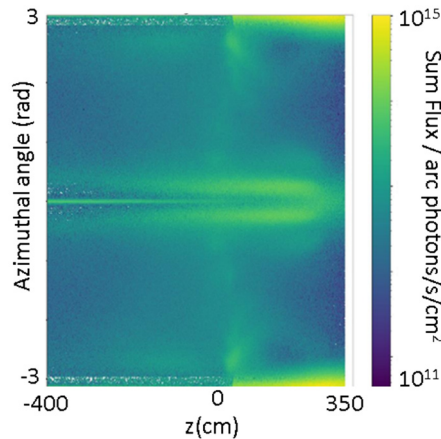


Figure 3: Photon flux as a function of azimuthal angle and position, z , along the beamline. The electron beam propagates from left to right, and the high flux regions at $\varphi=0^\circ$ and 180° are due to scattering of photons generated in the horizontal dipole.

The synchrotron radiation distribution has been calculated as elements are optimized. The beampipe design has evolved from a smooth 6 cm diameter tube to one with serrations along the horizontal axis for enhanced SR absorption, by expanding the beampipe to 13 cm wide and 10 cm high through the Q1eF quadrupole, and varying the final photon absorber position and geometry. Figure 4 shows flux incident on the beam-right IR vacuum chamber as a function of position for three potential final photon absorber (FPA) configurations.

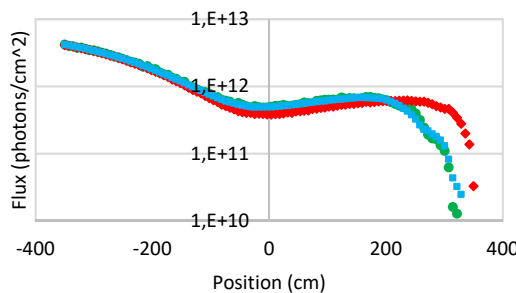


Figure 4: Simulated photon flux on the beam-right IR vacuum chamber vs. position z for circular FPA with diameter 4 cm located at: (blue) -380 cm extending to -345 cm, (green) -345 cm and zero length, and (red) -415 cm and zero length.

Synrad has a photon logging feature that yields a table of position, energy, flux and direction as a function of beam current. This output was used to simulate detector occupancy by propagating the photons through the beampipe

and into the detector array using using the Geant4 Monte-Carlo simulation packages integrated in the Fun4All framework [4-6].

Synchrotron radiation distributions have been calculated for 10 GeV electrons at 2.5A and 18 GeV electrons at 260 mA. The beam has been approximated using 90% of the beam in a narrow Gaussian distribution to approximate the central beam, and adding 10% of the beam with a wide Gaussian profile to better simulate the expected beam profile with extended tails. The Synrad simulations and detector background rates are yielding comparable values to an alternative program for calculating SR developed by Mike Sullivan at SLAC.

VACUUM SIMULATIONS

Molflow+, a complementary program to Synrad also developed at CERN, was used to model the vacuum of the EIC IR [3]. Molflow uses the same geometry files as Synrad, and by adding pumps and outgassing rates for the chamber materials, the pressure distribution in the beamline can be calculated. The vacuum in the EIC IR is critical, because in addition to SR induced backgrounds, scattering between the ion beam and the residual gas in the IR will yield nuclear scattering events, which are another undesirable detector background. The desired pressure in the IR is below 1×10^{-8} mbar during beam operations.

The IR will have ion pumps, non-evaporable getter (NEG) pumps, and cryopumping to evacuate the beamline during operation. Ion pumps use electrons trapped in a magnetic field to ionize gas, and DC voltage to accelerate the gas ions into plates where they implant and are removed from the vacuum space. This has the advantage of good pump speeds for noble gasses, but will be affected by detector magnets. NEG pumps have reactive metals which are heated under vacuum conditions to remove adsorbed gasses from the surface. The exposed reactive metal surface then chemisorbs gas incident on the surface. This has high pump speed for reactive gasses like hydrogen, but will not pump noble gasses, and requires a high temperature activation in-situ for optimal pumping.

Combination NEG/ion pumps use a NEG for high hydrogen pump speed and a small ion pump to handle the non-getterable gasses, and will be the primary appendage pumps in the IR. NEG material can also be deposited onto the surface of the vacuum chamber through sputter coating to provide distributed pumping through narrow beampipes [7], where extreme-high vacuum is critical [8], or in other areas where discrete pumps are insufficient. Finally, the cold bore beampipe inside magnet cryostats will pump through cryosorption, though when the surface saturates, the beampipe must be warmed to regenerate.

From the initial simulations, the vacuum in the IR chamber without beam (static vacuum) meets the goal of pressure of 1×10^{-9} mbar with 600 L/s combination NEG/ion pumps located at the pumping ports located about 4.5 m upstream and downstream of the IP. The simulated pressure distribution from the last electron dipole through the IP is shown in Fig. 5.

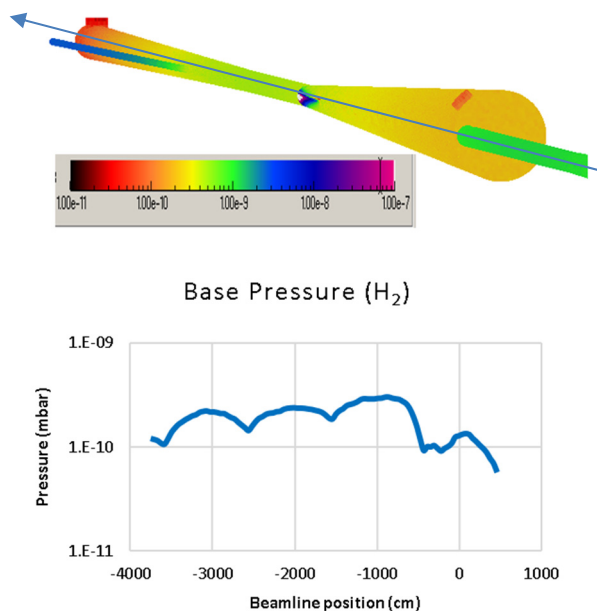


Figure 5: Hydrogen pressure distribution through the IR. The top figure shows the vacuum chamber as displayed in Molflow with the color scale corresponding to pressure and the arrow indicating electron beam direction. The graph shows a pressure profile along the axis of the electron beamline.

COUPLED SIMULATIONS

The EIC will undergo a period of commissioning prior to installation of the full detector packages. During this conditioning period, synchrotron radiation will cause significant outgassing from the vacuum system, including photon stimulated desorption and thermal desorption. To determine the pressure distribution in the IR as a function of beam dose, Synrad photon flux can be imported into Molflow.

Molflow includes tables of the expected hydrogen outgassing rates for materials such as copper or aluminium, as well as the outgassing rates for other gasses (see Fig. 6), as a function of photon flux. Using the Synrad flux per facet and the outgassing as a function of beam dose, Molflow can be used to determine the pressure distribution as a function of conditioning time and current.

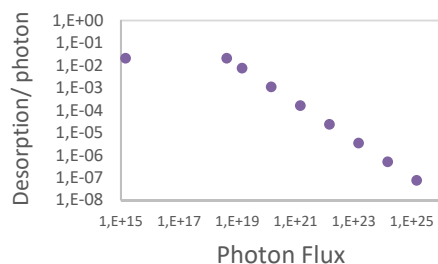


Figure 6: Estimated hydrogen desorption as a function of photon flux for an aluminum surface.

Two iterations of the pressure distribution for different conditioning times are shown in Fig. 7. The pressure drops with electron beam commissioning as expected, but for an aluminium chamber with only discrete pumping locations shows an unacceptably long time of 1 million Amp-hours, or operation over 40 years at 2.5 A, before reaching the goal pressure of 1×10^{-9} mbar. However, adding a distributed NEG coating to the system reduces this conditioning time to 50,000 hours or 2.5 years. Further optimizations will need to include the pumping due to the cryogenic beampipe in the magnet bores, consideration of the ion pump magnet interaction with the detector magnets, and updates to the interaction region geometry as the requirements change.

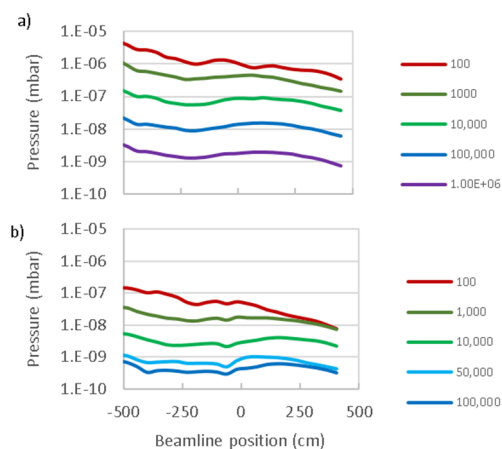


Figure 7: Hydrogen pressure distribution simulations as a function of conditioning time for a) an aluminum interaction region with combination NEG/ion pumps located at ± 4.5 meters and b) the same geometry but with added NEG coating to provide distributed pumping throughout the interaction region.

CONCLUSIONS

The EIC interaction region vacuum system is constrained by many factors to accommodate the detector systems and the beamline magnets. Synrad and Molflow are being used together to calculate detector backgrounds, both from SR-induced detector hits and beam-gas interactions due to SR-induced gas in the IR. These tools are allowing iterations on features such as the final photon absorber shape and position, the upstream beampipe dimensions and texture, pumping configuration and the expected pressure improvement attainable with a non-evaporable getter distributed pumping coating.

ACKNOWLEDGEMENTS

I would like to acknowledge the EIC IR background working group, with special thanks to Charles Hetzel for leading the design and Synrad modelling effort, Michael Sullivan for many design ideas and beam profile considerations, and Jin Huang for developing the interface between Synrad output and his detector background calculations.

REFERENCES

- [1] R. A. Khalek, “Science Requirements and Detector Concepts for the Electron-Ion Collider: EIC Yellow Report”, Mar. 2021. [arXiv:2103.05419](https://arxiv.org/abs/2103.05419)
- [2] H. Witte *et al.*, “The Interaction Region of the Electron-Ion Collider EIC”, presented at the 12th Int. Particle Accelerator Conf. (IPAC’21), Campinas, Brazil, May 2021, paper WEPAB002, this conference.
- [3] R. Kersevan and M. Ady, “Recent developments of Monte-Carlo codes Molflow+ and Synrad+”, in *Proc. 10th Int. Particle Accelerator Conf. (IPAC’19)*, Melbourne, Australia, May 2019, pp. 1327-1330.
[doi:10.18429/JACoW-IPAC2019-TUPMP037](https://doi.org/10.18429/JACoW-IPAC2019-TUPMP037)
- [4] S. Agostinelli *et al.*, “Geant4—a simulation toolkit”, *Nucl. Instrum. Methods Phys. Res., Sect. A*, vol. 506, pp. 250-303, Jul. 2003. [doi: 10.1016/S0168-9002\(03\)01368-8](https://doi.org/10.1016/S0168-9002(03)01368-8)
- [5] J. Allison *et al.*, “Geant4 developments and applications”, *IEEE Trans. Nucl. Sci.*, vol. 53, pp. 270-278, Feb. 2006.
[doi:10.1109/TNS.2006.869826](https://doi.org/10.1109/TNS.2006.869826)
- [6] J. Allison *et al.*, “Recent developments in Geant4”, *Nucl. Instrum. Methods Phys. Res., Sect. A*, vol. 835, pp. 186-225, Nov. 2016. [doi:10.1016/j.nima.2016.06.125](https://doi.org/10.1016/j.nima.2016.06.125)
- [7] T. Porcelli *et al.*, “NEG coating deposition and characterisation of narrow-gap insertion devices and small-diameter chambers for light sources and particle accelerators”, *Vacuum*, vol. 138, pp. 157-164, Apr. 2017.
[doi:10.1016/j.vacuum.2016.12.036](https://doi.org/10.1016/j.vacuum.2016.12.036)
- [8] M. L. Stutzman *et al.*, “Nonevaporable getter coating chambers for extreme high vacuum”, *J. Vac. Sci. Technol. A*, vol. 36, no. 3, p. 031603, May 2018.
[doi:10.1116/1.5010154](https://doi.org/10.1116/1.5010154)